Impacts of the Variability of Ice Types on the Decline of the Arctic Perennial Sea Ice Cover

Josefino C. Comiso

Cryospheric Sciences Branch, NASA Goddard Space Flight Center, Greenbelt MD USA 20771, email: josefino.c.comiso@nasa.gov

Abstract

The observed rapid decline in the Arctic perennial ice cover is one of the most remarkable signal of change in the Arctic region. Updated data now show an even higher rate of decline of 9.8% per decade than the previous report of 8.9% per decade mainly because of abnormally low values in the last 4 years. To gain insights into this decline, the variability of the second year ice, which is the relatively thin component of the perennial ice cover, and other ice types is studied. The perennial ice cover in the 1990s was observed to be highly variable which might have led to higher production of second year ice and may in part explain the observed ice thinning during the period and triggered further decline. The passive microwave signature of second year ice is also studied and results show that while the signature is different from that of the older multiyear ice, it is surprisingly more similar to that of first year ice. This in part explains why previous estimates of the area of multiyear ice during the winter period are considerably lower than the area of the perennial ice cover during the preceding summer. Four distinct clusters representing radiometrically different types have been identified using multi-channel cluster analysis of passive microwave data. Data from two of these clusters, postulated to come from second year and older multiyear ice regions are also shown to have average thicknesses of 2.4 and 4.1 m, respectively, indicating that the passive microwave data may contain some ice thickness information that can be utilized for mass balance studies. The yearly anomaly maps indicate high gains of first year ice cover in the Arctic during the last decade which means higher production of second year ice and fraction of this type in the declining perennial ice cover. While not the only cause, the rapid decline in the perennial ice cover is in part caused by the increasing fractional component of the thinner second year ice cover that is very vulnerable to total melt due to warming in the Arctic, especially in spring.

1. Introduction

The Arctic has been the focus of many climate change studies because change signals are expected to be amplified in the ice covered region primarily through the ice-atmosphere albedo feedback. Satellite data have been used to show declines in the extent and area of the hemispherical sea ice cover but from November 1978 through 2005, the rate has been quite modest at about 2 to 3% per decade (Parkinson and others, 1999; Comiso, 2004). Also, using available submarine (but sparse) upward looking sonar data from the 1950s to the present, substantial reductions in average thickness have been observed

(Rothrock and others, 1999; Wadhams and Davis, 2000). The most intriguing signal in the region so far is the relatively rapid 9.8% per decade decline in the perennial sea ice cover from 1978 to 2005. The perennial sea ice cover is that which survives the summer melt and consists mainly of thick multiyear ice floes that are the mainstay of the Arctic sea ice cover. The perennial ice cover is also key to the ice-albedo feedback effects that make the Arctic an especially good region to detect early signals of a possible warming associated with increasing greenhouse gases in the atmosphere. It is thus important that the observed change in the perennial ice cover is studied in greater detail.

The extent and area of the perennial sea ice cover can be studied quantitatively with reasonably good accuracy using passive microwave data. The characteristics of the perennial ice are derived from microwave data at the end of the summer melt in mid-September (i.e., during ice cover minimum) when the surface of the ice cover has basically dried up and the microwave emissivity of the surface is relatively stable. Thus, the usual problem of interpretation of the signature of ice during the mid summer period when the latter is affected by the presence of melt ponds and wet ice surfaces is not so relevant. During the ensuing winter, the spatial extent and distribution of the perennial ice cover undergo many changes associated with wind, ocean current, tides, advection, storms and other factors. Such changes are important to monitor since they are key to an understanding of the processes that lead to the distribution of the perennial ice cover in the subsequent summer. In this paper, we take advantage of known differences in the microwave signature of multiyear year ice and first year ice to gain some insights into this phenomenon. We also take advantage of the multi-channel capability to assess ability to discriminate different ice surfaces that may have different thicknesses. Ability to identify such surfaces would also enable an improved interpretation of submarine thickness data and data from IceSAT and CryoSAT.

2. Multichannel Microwave Signature of Arctic ice types

Arctic inhabitants (e.g., Innuits) have been using multiyear ice floes as sources of drinking water for a long time and they also knew that seasonal ice is too salty to be used for the same purpose. The difference in salinity turns out to be the key factor that makes the passive microwave signatures of first year so different from that of multiyear ice floes (Vant and others, 1974). Because of the presence of brine in first year ice, the imaginary part of the dielectric constant is relatively high and the material becomes opaque or lossy. This means that the effective emissivity of first year ice is high since the microwave signal comes from top surface layer of the ice (<1 cm) and subject only to little or no scattering. On the other hand, since multiyear ice is basically fresh ice, the absorption coefficient is low, and the material is transparent with the microwave signal coming from several tens of centimeters from the surface of the ice. The effective emissivity of multiyear ice is thus relatively low since a large fraction of this signal is scattered primarily by air pockets and other inhomogeneities

within the ice. In essence, this explains why the brightness temperature of multiyear ice is significantly lower than that of first year ice. Since the efficiency of scattering is dependent on the wavelength of the radiation and the size (and number) of scatterers, the emissivity of multiyear ice is frequency dependent and is low when the radiation that is comparable to the size of the scatterers. But while the emissivity of first year ice is relatively well defined, the emissivity of multiyear ice is much more variable because the size and number of scatterers within the ice varies from one ice floe to another depending on the history of the ice itself. Such spatial variability in the signature of multiyear ice has been observed through direct measurements in various parts of the Arctic that were accessible by ship (Grenfell, 1992). Aircraft measurements have also confirmed this variability (Comiso and others, 1990) and in some cases the signature of second year ice was even found to be different from that of the older ice types (Tooma and others, 1975). The transformation from first year to second year occurs mainly in the summer and in part caused by meltponding and brine drainage. It is thus reasonable to expect that the signature of second year ice may be different from that of the older ice types which have gone through a few summers.

2.1 Time Series for Different Years

Although the extent and area covered by perennial sea ice in the Arctic have been declining rapidly, i.e., 8.2 and 9.8 % per decade (Comiso, 2005,in press) for extent and area, respectively, the interannual variability is large as indicated in Figure 1a. The plots show a slowly declining perennial ice cover in the 1980s, a sudden drop from 1989 to 1990, a large yearly variability from 1991 to 1997 and a more monotonic decline from 1998 to the present. The large interannual variability in the 1990s is interesting in that an increase in the area of the perennial ice cover from one year to another could only happen if the production of second year ice exceeds the loss of multiyear ice through melt and advection out of the Arctic region (e.g., through Fram Strait). On the other hand, a decrease in perennial ice cover would mean decreases in both second year ice and older ice types. A repetition of this process from 1991 to 1997 would therefore lead to increases in the fraction of second year ice floes which are generally thinner than the older ice types. It is intuitive to postulate that the decreases in the extent and area of the perennial ice since 1997 are in part due to the presence of a larger percentage of second year ice which is more vulnerable to summer melt than the older and thicker ice types. We use passive microwave data to gain insights into this phenomenon.

Because of the general inaccessibility of the Arctic, it has not been easy to do surface measurements to establish regional variations in the emissivity of multiyear ice. As mentioned earlier, aircraft measurements by Tooma et al (1975) revealed signatures for some ice floes that are intermediate to those of first year ice and the older multiyear ice types. These ice floes have been examined using coincident laser and infrared data and postulated to be second year ice floes. Although the ability to

discriminate and monitor second year ice is important, progress on the study of the signature of second year ice has been slow mainly because of the difficulty of identifying such ice floes unambiguously within the pack. To get an idea about how second year ice could be studied using satellite data, we take advantage of historical data and look into the time periods when the production of second year ice floes was likely very high. We refer to the big increase in the perennial ice area from 1995 to 1996 as shown in Figure 1a. Color coded ice concentration maps during minimum extents in 1995 and 1996 are shown in Figures 1b and 1c, respectively, while a color coded map of the difference is presented in Figure 1d. The difference map clearly indicate the locations where the ice cover has advanced considerably (i.e., blues and greens) from the previous year. Using satellite infrared data, it was also observed that the same general area went through anomalously cold temperatures during the winter period from late 1995 to early 1996 (Comiso and others, 2003). Such cold temperatures may have facilitated ice growth and allowed ice in the region to grow thick enough to be able to survive the summer melt.

The average brightness temperatures (T_B) within a 5 by 5 pixel study area (in white box in Figure 1d) located in the blue region (which we will assume to represent second year ice) as well as those in the seasonal and traditionally multiyear ice regions (see green and black boxes) were calculated for each daily data from September through March the following year and the results are plotted in Figure 2a, 2b, and 2c, for 37 GHz (V), 37 GHz (H), and 19 GHz (V), respectively, with V and H indicating vertical and horizontal polarization. The plots in blue lines, which represent seasonal region, are shown to have open water signatures in September but during freeze-up, the signatures at all three frequencies quickly increased to the typical FY ice signature in early December. The plots for multiyear ice (black line) show that from September through March the signatures are considerably lower than those of FY ice and appear almost constant during the entire period indicating the stability of the signature in the region. The signatures of second year ice (red line) are shown to be higher than those of multiyear during the period and lower than those of FY ice. However, in mid-November, there is a slight increase for both 37 GHz (V) and 37 GHz (H) channels and the final value gets closer to (but lower than) those of FY ice. The values for the 19 GHz (V) channel also went up but earlier than those of the other frequency. Some fluctuations in the T_B for ice covered surfaces at all channels are evident and may be caused by lead formation due to tides, wind, and storms, and/or by sudden changes in surface temperature. Because the ice cover is dynamic the variations in T_B may also be caused by ice floes getting in and out of the study region. Considering that a typical ice drift velocity is about 8 km per day, not necessarily in the same direction, and the size of the study areas is 125 by 125 km, the effect of dynamics has to be gradual since it would take a few weeks for an ice floe to get advected in and out of the study box.

That the signature of second year ice appears considerably higher than that of the older multiyear ice and gets even close to that of first year

ice during the winter months is interesting since it provides an indication that one summer may not be enough to completely desalinate first year ice. This may also explain observed discrepancies in the areal extents of the perennial ice cover and the derived multiyear ice cover in subsequent winter. The observed increase in the T_B during the winter period is not totally unexpected. Such a change cannot be attributed to surface temperature since the signature would go down as the surface gets colder in late autumn and winter. A more plausible explanation is the introduction of new and young ice during the freeze-up period. Being near the ice edge in the summer, the study region is vulnerable to divergences that can cause the formation of large leads and when followed by a refreezing of the surface will cause an increase in the concentration of FY ice. Strong winds that cause such divergence could also directly impact the signature of second year ice by causing flooding followed by refreezing at the snow ice surface. Also, because they are generally thinner, second year ice has freeboards that are more vulnerable to flooding than the older ice types. The intrusion of sea water into the snow ice interface would increase surface salinity and therefore the brightness temperature of the surface, following aforementioned discussion.

It is also interesting to note that in each study area, the time variation in signatures at the various frequencies and polarizations are highly correlated although the magnitude of the change are not the same. It is apparent that the increase in the T_B of second year ice at 19 GHz (V) is more gradual and started earlier that those of the 37 GHz channels. The overall increase in T_B may thus be a combination of separate events that started early but was not sensitive enough to the 37 GHz radiation until the middle of November.

For comparison, an example showing a more modest increase in the perennial ice cover such as that from 2002 to 2003 was also analyzed. The ice concentration during ice minima in 2002 is shown in Figure 3a while the brightness temperatures at 18 GHz in a subsequent winter month (March 2003) is shown in Figure 3b. The outline of the multiyear ice pack as detected by the passive microwave sensor is apparent in Figure 3b as reduced brightness temperature which decreases towards the north. It is also apparent that the effect of ice drift in this case is relatively minor since the location of the multiyear ice pack in March is generally similar to that of the perennial ice as detected in the previous summer (Figure 3a). The ice concentration during ice minima in 2003 is shown in Figure 3c and indicates significantly more ice towards the Novaya Zemlya Island than in 2002. The difference map shown in Figure 3d again provides a quantification of the extent in the advance of the ice cover (in blue) towards the region. The time series of T_B images provide a means to monitor large scale changes in the location (or movements) of the multiyear ice cover. The March image in Figure 3b and subsequent images indicate that it is unlikely that multiyear ice had been advected to the second year ice (blue) region. The general region was again the site of anomalously cold temperatures during the winter months as indicated by satellite AVHRR data in Figures 3e and 3f. The region, which is usually

a seasonal ice region, is thus likely an area of thick first year ice cover that can survive the summer melt. It is thus plausible to assume that the area of advance (in blue) as indicated in Figure 3d is mainly covered by second year ice floes in 2003. The average brightness temperatures of a 5 by 5 pixel area in the middle of the blue region from September to March is presented in Figure 4, together with those from the seasonal and multiyear ice regions identified in Figure 1. In this case, the signature of the second year ice is even closer to that of the first year ice signature and basically overlaps with that of the latter in mid-winter period. This may be in part because the region is adjacent to the Atlantic Ocean making the ice cover even more vulnerable to big waves, divergence and flooding than the previous example. Also, the blue region is quite small compared to the other example and the likelihood for contamination by first year ice by advection is higher.

2.2 Cluster Analysis

The time series study presented in the previous section indicates that while the signature of second year ice appears to be intermediate to that of the older multiyear ice and first year ice, it is difficult to monitor the same surface during the winter period because of changing signatures that may be associated with changing fraction of contamination by first year ice types. It is, however, encouraging to note that the signature of some types of multiyear ice is basically stable throughout the winter period. Because the passive microwave data set is a multi-channel data set, with each channel providing correlated but different information we examine how several channels can be used in concert to study potentially different multiyear ice types within the consolidated ice region of the Arctic in winter. Figure 5a shows a 3-D scatter plot of Arctic passive microwave brightness temperature data in March 2003 using the 19 GHz (V), 37 GHz(V), and 89 GHz (V) channels. The respective 2-D projections of the main 3-D plot are also shown. The data points that represent consolidated ice regions are the relatively compact clusters labeled A, B, C, and D. Similar clustering of data points in the Arctic region during winter have been noted previously using historical passive microwave data (Comiso, 1995). It is remarkable that unique clustering of the data points tend to reappear during every winter period. The persistence of these clusters is a strong indication that the data points represent surface (not the atmospheric) properties and that data from the same cluster are likely associated with similar types of surfaces. We already know that data points in cluster A represents first year ice types or ice located in the seasonal sea ice region. Because of proximity to the first year ice cluster and following the results of Tooma et al. (1975), we postulate that data points in cluster B correspond mainly to second year ice floes. The C and D clusters are also postulated to represent the older multiyear ice types. By virtue of location of the data points, we also postulate that the data points in C are relatively younger that those in D. The data points corresponding to the D cluster are actually located in the area north of Greenland and the Canadian Archipelago and where the oldest ice types

(6 years and older) are expected to be found (Colony and Thorndike, 1988). If scattering is the primary mechanism for the different signatures, it makes sense that the emissivity of data points in cluster B is lower than those in cluster A while those of C and D are lower than those of B. The aging process usually leads to alterations in the size and number of air pockets which are the primary scatterers within the ice. For completeness, the other data points have been labeled E, representing new ice and/or mixtures of thick ice and open water and O, representing open water. Also, for comparison, the same data set are plotted in Figure 5b, but using a combination of a different set of channels. In this case 37(H) data are used instead of 89 GHz(V), where H stands for horizontal polarization. It is encouraging that the same 4 clusters identified in Figure 5a are also revealed in this set of data although the separation of the clusters are not as distinct.

In a 3-D space, the clusters are like ellipsoids with the x, y, z axis representing the variability in each of the channels. It appears that the axis with the highest variability correspond to the channel with the highest frequency confirming that the main cause of variability is scattering. The size and variability of clusters representing each type are not any more compact than those shown because of spatial variability in the characteristics of the material including it's snow cover and temperature. It is, however, evident that for optimal separation of the clusters, the right set of channels has to be used.

To illustrate how the passive microwave multi-channel data can be utilized for ice-type mapping of the Arctic region, Figure 6a is a color coded map representing radiometrically different ice types based on the different clusters identified in the 3-D plots in Figure 5. The four distinct clusters for consolidated ice are represented in the expected geographical locations with cluster A data points (in gold) being mainly located at the seasonal ice region, cluster B data points (orange) at the periphery of the perennial ice area and clusters C (in yellow) and D (in green) data points in the interior of the pack where the older ice types are expected to be located. The distribution of radiometrically different ice types as presented in Figure 6a provides an added dimension in the study of sea ice cover. Ability to generate this map consistently would provide a powerful means of monitoring different types of multiyear ice cover and gaining a good understanding of the cause of the observed variability in the perennial ice cover.

For comparison, a similar analysis using data in April 1994 is presented in Figure 6b. The data in Figure 6b is especially useful because submarine sonar thickness data (provided by Peter Wadhams, private communications, 2004) were acquired in April 1994 and it provided the opportunity to compare the cluster result with the average thickness of some of the ice floes within the cluster. The average ice thickness over 50 km segments were estimated from sonar data to be 2.48, 2.55, and 4.14 m, over the locations indicated in the map as solid black triangle, circle, and square, respectively. Two data points belong to cluster B which is color coded in orange in the map and have average thicknesses equal to

what would be expected as the likely thickness of second year ice (i.e., about 2.5 cm). It is also interesting that the average thickness of ice in the inner section (yellow) is significantly higher than that of the other two data points. This result is an indication that the multichannel passive microwave data contains some thickness information. Having this additional information from the same sensor that provides ice extent and area would make the data set considerably more useful for studying sea ice mass balance processes. Further validation is, however, required and since submarine sonar data are not so readily available, the use of ICESat and CryoSat data (when available) would be very important for this purpose. Coincident measurements from the ground of the physical and radiative characteristics of ice from the different clusters would also be highly desirable for accurate interpretation of the data.

3 Multiyear Ice Cover Variability

The cluster analysis is one good way for utilizing the multichannel passive microwave data for studying the temporal and spatial variability of radiometrically different multiyear ice surfaces in the winter. Unfortunately, the technique has not matured to the point where surfaces belonging to the same clusters can be consistently identified. Part of the reason is the overlapping signatures of the different surface types and changes associated with the changing environmental conditions during the season. One parameter that can be useful for interpreting the variability of the multiyear ice cover is multiyear ice concentration. Such parameter has been derived by Gloersen et al. (1992) and Johannessen et al. (1999) by using a mixing algorithm and assuming that the signature of multiyear ice is constant with time and space. Although we know that this is not the case (Grenfell, 1992), the derived multiyear ice distribution still provide useful information about spatial changes in the distribution of multiyear ice during the winter period. In this study, such parameter has been generated using a modified version that makes use of a dynamic set of tie points that account for temporal changes during each winter period. The resulting multi-year ice concentration maps corresponding to the same set of data presented in Figure 6a and 6b are shown in Figures 6c and 6d, respectively. The multi-year ice concentration maps do not show real multiyear ice concentrations but the general spatial location of the multiyear ice cover is approximately right during the dry winter months. Where the multiyear ice concentrations are low, it may be important to remember that ice in the regions may be primarily second year ice with much higher concentrations.

To illustrate how the derived multiyear ice concentration maps could be utilized in Arctic sea ice mass balance studies, plots of the extent and area of the multiyear ice cover and also the perennial ice cover from 1979 to 2005 are presented in Figure 7. It is remarkable that the extents of the retrieved multi-year ice cover are consistent, at least in magnitude, to those of the perennial ice cover. The good agreement in the extents is an illustration that the two data sets are providing information about the same features of the ice cover. It is also notable that the area of the

derived multiyear ice cover in winter differs substantially (as much as $2 \times 10^6 \, km^2$ lower) from that of the perennial ice cover. Similar discrepancies between the perennial ice area and the area covered by multiyear ice in mid winter have been reported by Kwok (2004) using QuickSCAT and SAR data. The large differences in ice area are mainly caused by the unrealistic assumption that the signature of multiyear ice floes is unique and the variations in signature are simply due to different mixtures of multiyear and first year ice floes. The in situ studies by Grenfell (1992) show that this is not the case and furthermore, the cluster analysis indicates the existence of radiometrically different surface types. Also, the multiyear ice concentration maps do not properly represent the second year ice cover, the signature of which may be very close to that of first year ice. In the Kwok (2004) study, there was no mention of the possibility that the backscatter of second year ice may be different from that of the older multiyear ice type. Since such difference in signature appears to exist with the passive microwave data, a similar case is likely with active microwave data. The discrepancy between the summer and winter ice area is in part attributed to ice transport, especially through the Fram Strait region, which can account for approximately $1 \times 10^6 \, km^2$ a year.

Trend analyses also show that the trend in area and extent using multiyear ice concentration data are comparable to those from the perennial ice data. Similar results for multiyear ice cover in winter were also reported by Johannessen et al. (1999) who also used a mixing algorithm similar to that described above. The interannual variabilities are sometimes correlated but other times, they are not. The lack of correlation in extent for some years may be caused by storms that redistribute the ice cover and enhance the extent but not the ice area.

To provide additional insight into the possible impact of the changing composition of the perennial ice cover, the yearly anomalies of the perennial ice are presented in Figure 8. The yearly anomalies do not provide probable locations of second year ice cover as in the year-to-year differences shown in Figure 1 and 3 but they provide the means to assess how the extent of the first year ice cover has been evolving. It is the first year ice that becomes second year ice and as the fraction of first year ice increases in the Arctic basin, the production of second year ice is likely to increase. The anomaly maps show a dominance of positive anomalies in the 1980s confirming that the perennial ice cover was relatively extensive during the period. In the 1990s, negative anomalies are dominant, except for 1992, 1994, and 1996. In the 2000s, including 2004 and 2005 (which are not shown for lack of space), negative anomalies were even more dominant than in the 1990s. The rate of decline actually accelerated during the last four years because the average area of the perennial sea ice cover dropped to about $4.9 \times 10^6 \, km^2$, which is 14% lower than the overall average of $5.7 \times 10^6 \, km^2$ for all data from 1979 to 2005. Declines in the perennial ice cover translate directly to increases in the area of seasonal ice. This would in turn cause increases in the production of second year ice the following year if cooling is sustained during the winter period.

4. Discussion and Conclusions

The Arctic perennial ice cover has been declining rapidly while concurrently, the average surface temperature has been increasing. However, the hemispherical ice cover for all seasons has been declining only moderately and the trends in winter temperatures in many parts of region are negative. Moreover, the data record is relatively short and in light of the observed variability of the Arctic climate system associated with Arctic Oscillation (Thompson and Wallace, 1998) and periodic changes in wind circulation (Proshutinsky and Johnson 1997) it is difficult assess what is really going on. There are however indications that the changes are basically linear during the last two decades (Overland and Wang, 2005). Detailed examination of the possible environmental reasons for the large decline in the perennial ice cover is thus important.

The decline can be associated with an overall thinning of the ice cover as has been observed by limited historical submarine sonar data. Such thinning, however, may in part be caused by changes in the fractional composition of the different multiyear ice types including second year ice, as opposed to direct thermodynamics effects. This study shows that during the last twenty five years, there were episodes of large interannual variability in the ice cover that could have led to higher fraction in the relatively thin second year ice type and therefore the observed thinning in the ice in the 1990s. Such variations may have also triggered the almost monotonic decline in the perennial ice cover since 1998. Declines in the perennial ice cover leads to increases in the fraction of first year/seasonal ice in the Arctic basin. Such increase leads to increases in the formation of second year ice which is a component of the observed second year ice cover. Increases in the second year ice component would in turn reduce the average thickness of the perennial ice cover making the latter even more vulnerable to summer melt.

The multi-channel signature of second year ice was also observed to be different from that of the older multiyear ice types. It also appears that the signature approaches that of first year ice in some cases which is an indication that the second year ice may still have significant salt content. The different signature may also be reflected as biases in the assessment of multiyear ice area in winter using not only passive but also active microwave data. This may explain the large discrepancy of the area of perennial ice when compared to the area of multiyear ice inferred in subsequent winter using various techniques (e.g., Kwok, 2004).

Cluster analysis using multichannel data provides additional information about radiometrically different surface types. At least four different clusters in the consolidated ice region in winter have been identified. Submarine sonar measurements of two of these ice types have been identified to have significantly different ice thicknesses. With more validation, this would mean that the passive microwave data provide information about ice thickness which in conjunction with other data sets would be very useful for sea ice mass balance studies.

Yearly anomalies of the perennial ice cover provide the means to examine where the perennial ice has been retreating and where they have been advancing. Consistent retreat is apparent since the large anomaly in 1998 which may have been triggered by relatively high production of second year ice the previous period. The basically monotonic decrease in the perennial ice cover from 1998 to the present means more first year ice production in the Arctic basin which in turn means higher production of second year ice, assuming that the winter periods stay relatively cold. The effects of other factors are likely important but the impact of variations in the ice types cannot be overlooked.

References:

Colony, R. and A. Thorndike. 1985. Sea ice motion as a drunkard's walk. *J. Geophys. Res.*, **90**, 965-974.

Comiso, J.C., Arctic warming signals from satellite observations. *Weather* (submitted, 2005).

Comiso, J. C. 2003. Warming Trends in the Arctic. *J. Climate* , **16**(21), 3498-3510.

Comiso, J. C., 2002. A rapidly declining Arctic perennial ice cover. *Geophys Res. Letts., 29(20), 1956, doi:10.1029/2002GL015650.*

Comiso, J.C., and R. Kwok. 1996. The summer Arctic sea ice cover from satellite observations, *J. Geophys. Res.,* **101**(C2), 28397-28416.

Comiso, J.C., P. Wadhams, W. Krabill, R. Swift, J. Crawford, and W.Tucker. 1991. Top/Bottom multisensor remote sensing of Arctic sea ice, *J. Geophy. Res., 96*(C2), 2693-2711.

Comiso, J.C., J. Yang, S. Honjo, and R.A. Krishfield. 2003. The detection of change in the Arctic using satellite and buoy Data. *J. Geophys. Res.* **108**(C12), 3384, doi:1029-2002jc001247, 2003.

Kwok, R. 2004. Annual cycles of multiyear sea ice coverage of the Arctic Ocean: 1999-2003, *J. Geophys. Res.,* **109** (C11004), doi:10.1029/ 2003JC002238.

Kwok, R., J.C. Comiso, and G. Cunningham. 1996. Seasonal characteristics of the perennial ice cover of the Beaufort Sea, *J. Geophys. Res.,***101**(C2), 28417-28439.

Gloersen P., W. Campbell, D. Cavalieri, J. Comiso, C. Parkinson, H.J. Zwally. 1992. Arctic and Antarctic Sea Ice, 1978-1987: Satellite Passive Microwave Observations and Analysis, *NASA Spec. Publ. 511.*

Grenfell, T.C. 1992. Surface-based passive microwave studies of multiyear ice. *J. Geophys. Res.,* **97**(C3), 3485-3501.

Johannessen, O.L., E.V. Shalina, and M.W. Miles. 1999. Satellite evidence for an Arctic sea ice cover in transformation. *Science*, **286**, 1937-1939.

Overland, J.E., and M. Wang. 2005. The Arctic climate paradox: The recent decrease of the Arctic Oscillation. *Geophys. Res. Lett.*, **32**, l06701, doi:10.1029/2004/GL021752.

Parkinson, C.L., D.J Cavalieri, P. Gloersen, H.J. Zwally, and J.C. Comiso. 1999. Arctic sea ice extents, areas, and trends, 1978-1996, *J.*

Geophys. Res., **104**(C9), 20837-20856.

Proshutinsky, A.Y. and M.A. Johnson, 1997. Two circulation regiomes of the wind driven Arctic Ocean, *J. Geophys. Res.,* **102**, 12,493-12,514.

Rothrock, D.A., Y. Yu, and G. Maykut. 1999. Thinning of the Arctic sea-ice cover, *Geophys. Res. Lett.*, **26**, 3469-3472.

Thompson, D.W.J., and J.M. Wallace. 1998. The Arctic oscillation signature in the wintertime geopotential height and temperature fields, *Geophys. Res. Lett.*, **25,** 1297-1300.

Tooma, S.G., R. A. Mennella, J.P. Hollinger, and R.D. Ketchum, Jr. 1975. Comparison of sea-ice type identification between airborne dual-frequency passive microwave radiometry and standard laser/infrared techniques, *J. Glaciol.,* **15**(73), 225-238, 1975.

Vant, M.R., R.B. Gray, R.O. Ramseier, and V. Makios. 1974. Dielectric properties of fresh and sea ice at 10 and 35 GHz, *J. Applied Physics*, **45**(11), 4712-4717.

Wadhams, P. and N.R. Davis. 2000. Further evidence of ice thinning in the Arctic Ocean, *Geophys. Res. Lett., 27,* 3973-3976.

List of Figures:

Figure 1. (a) extent and area of the perennial ice cover from 1979 to 2005; (b) ice concentration map during ice minimum in 1996; (c) ice concentration map during ice minimum in 1995; (d) difference of the ice concentration maps of 1996 and 1995.

Figure 2. Brightness temperatures in three study areas for (a) 37 GHz (V); (b) 37 GHz (H); and (c) 19 GHz (V). The study areas are in seasonal region (blue), probable second year ice region (red), and multiyear ice region (black).

Figure 3. (a) ice concentration map during ice minima in 2002; (b) brightness temperature at 18 GHz(V) in March 2003; (c) ice concentration map during ice minima in 2003; (d) difference map of the ice minima in 2003 and 2002; (e) surface temperature from AVHRR IR data in January 2003; and surface temperature from AVHRR IR data in March 2003.

Figure 4. Brightness temperatures in three study areas for (a) 37 GHz (V); (b) 37 GHz (H); and (c) 19 GHz (V). The study areas are in seasonal region (blue), probable second year ice region (red), and multiyear ice region (black).

Figure 5. Cluster maps using multichannel passive microwave data in (a) March 2003 and (b) April 1994. The color code are labeled to correspond to the various clusters identified in the scatter plots shown in Figure 2. The thickness of ice in April 1994 was measured by upward looking sonar on board a submarine and the thickness is shown to change from around 2.5 m in the cluster B region to 4.1 m in the cluster C region.

Figure 6. Maps of ice types based on cluster analysis for (a) March 2003;
and (b) April 1994. Maps of multiyear ice concentration for (c) March
2003; and (d) April 1994.
Figure 7. Plots of extent (blue) and area (pink) of the multiyear ice cover
and extent (dark blue) and area (red) of the perennial ice cover.
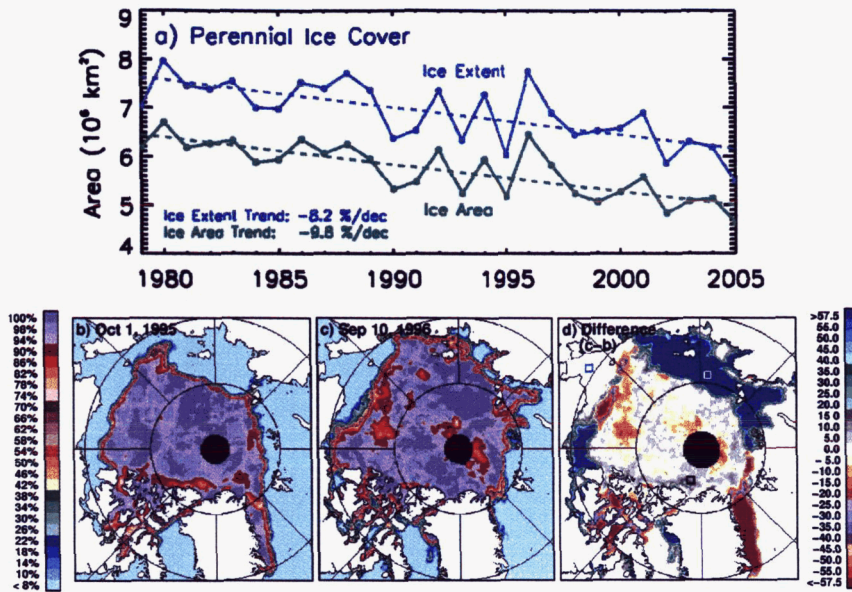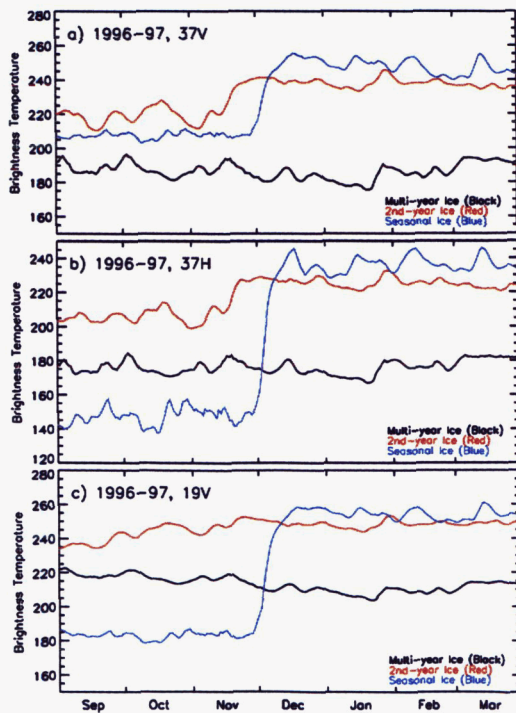Figure 8. Anomaly maps of the perennial ice cover from 1979 to 2003.
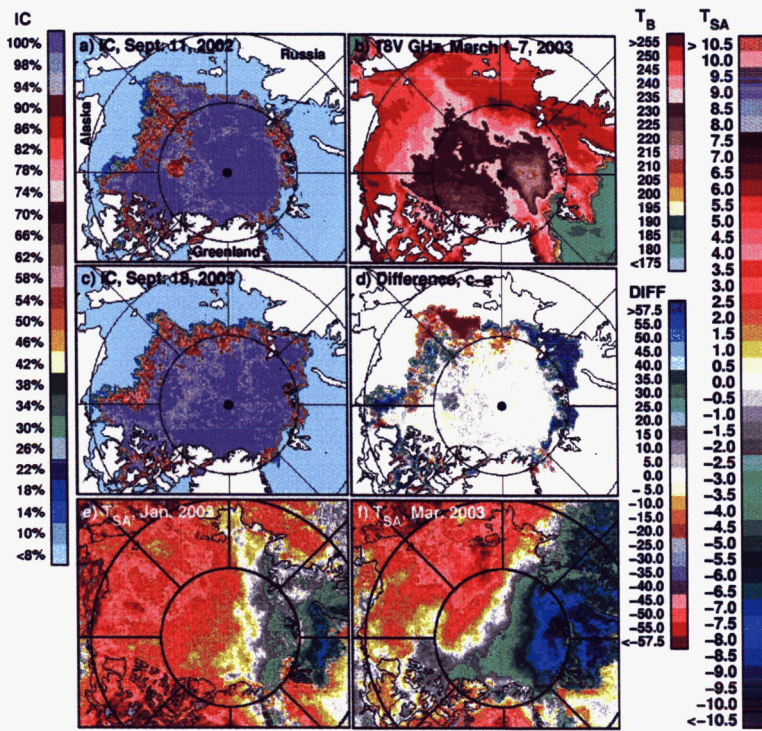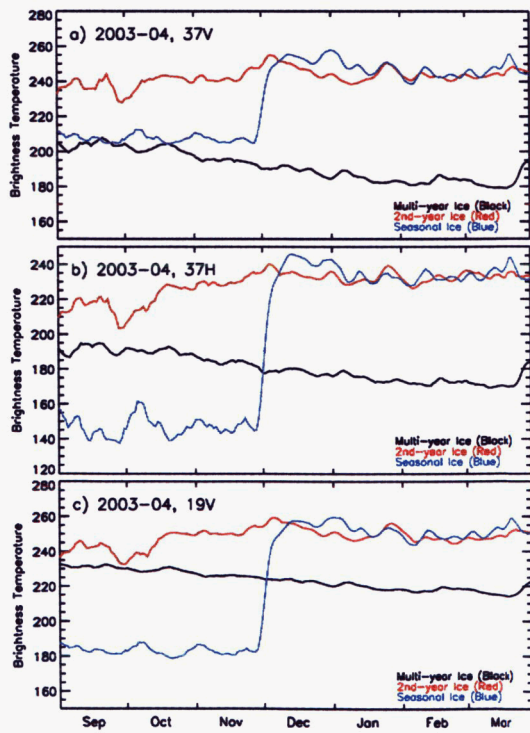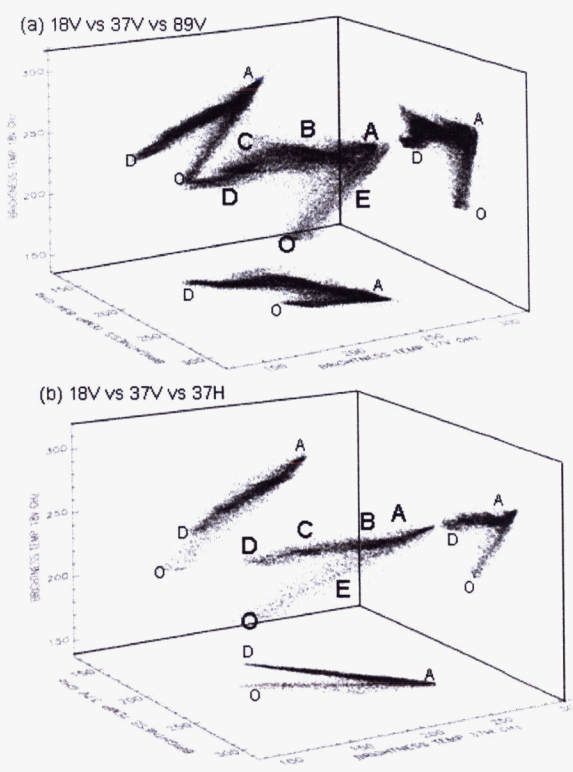

Figure 1.

Figure 2.

Figure 3.

Figure 4

(a) 18V vs 37V vs 89V

(b) 18V vs 37V vs 37H

Figure 5.

a) March 2003

b) April 1994

c) March 2003
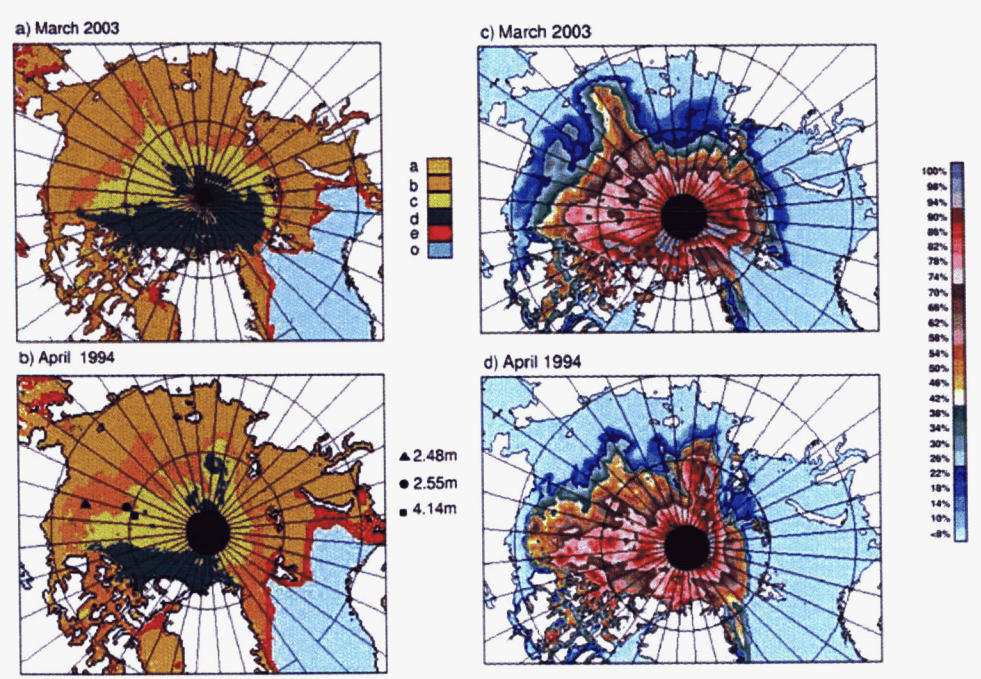
d) April 1994

▲ 2.48m
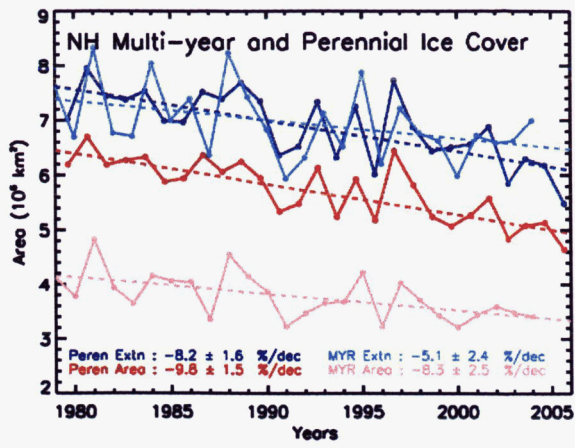● 2.55m
■ 4.14m
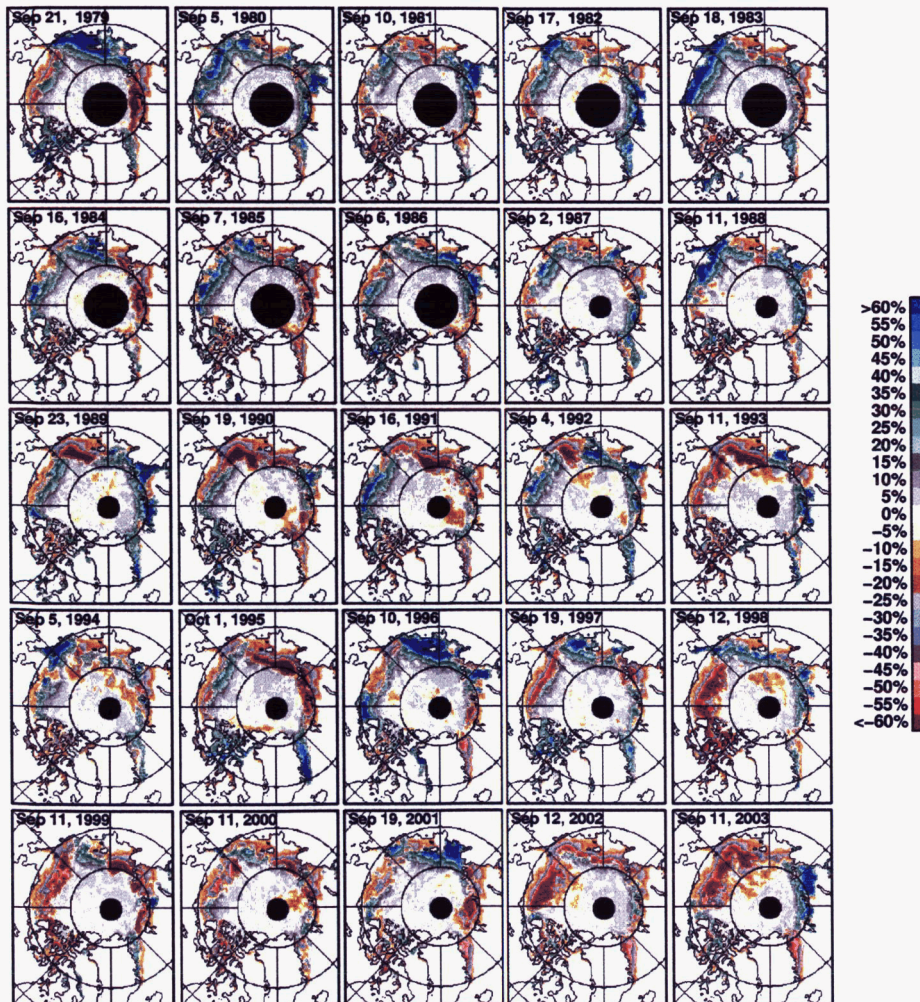
Figure 6.

Figure 7.

Figure 8.

Title: Impacts of the Variability of Ice Types on the Decline of the Arctic Perennial Sea Ice Cover

Author: Josefino C. Comiso
Cryospheric Sciences Branch, Code 614.1
email: josefino.c.comiso@nasa.gov

Abstract
The observed rapid decline in the Arctic perennial ice cover is one of the most remarkable signal of change in the Arctic region.   Updated data now show an even higher rate of decline of 9.8% per decade than the previous report of 8.9% per decade mainly because of abnormally low values in the last 4 years. To gain insights into this decline, the variability of the second year ice, which is the relatively thin component of the perennial ice cover, and other ice types is studied. The perennial ice cover in the 1990s was observed to be highly variable which might have led to higher production of second year ice and may in part explain the observed ice thinning during the period and triggered further decline. The passive microwave signature of second year ice is also studied and results show that while the signature is different from that of the older multiyear ice, it is surprisingly more similar to that of first year ice. This in part explains why previous estimates of the area of multiyear ice during the winter period are considerably lower than the area of the perennial ice cover during the preceding summer. Four distinct clusters representing radiometrically different types have been identified using multi-channel cluster analysis of passive microwave data. Data from two of these clusters, postulated to come from second year and older multiyear ice regions are also shown to have average thicknesses of 2.4 and 4.1 m, respectively, indicating that the passive microwave data may contain some ice thickness information that can be utilized for mass balance studies. The yearly anomaly maps indicate high gains of first year ice cover in the Arctic during the last decade which means higher production of second year ice and fraction of this type in the declining perennial ice cover. While not the only cause, the rapid decline in the perennial ice cover is in part caused by a higher component of the thinner second year ice cover that is more vulnerable to the warming in the Arctic, especially in spring.